

Measurement of the top quark mass in the dilepton channel using m_{T2} at CDF

T. Aaltonen,²⁴ J. Adelman,¹⁴ B. Álvarez González,^{12,w} S. Amerio,^{44b,44a} D. Amidei,³⁵ A. Anastassov,³⁹ A. Annovi,²⁰ J. Antos,¹⁵ G. Apollinari,¹⁸ A. Apresyan,⁴⁹ T. Arisawa,⁵⁸ A. Artikov,¹⁶ J. Asaadi,⁵⁴ W. Ashmanskas,¹⁸ A. Attal,⁴ A. Aurisano,⁵⁴ F. Azfar,⁴³ W. Badgett,¹⁸ A. Barbaro-Galtieri,²⁹ V. E. Barnes,⁴⁹ B. A. Barnett,²⁶ P. Barria,^{47c,47a} P. Bartos,¹⁵ G. Bauer,³³ P.-H. Beauchemin,³⁴ F. Bedeschi,^{47a} D. Beecher,³¹ S. Behari,²⁶ G. Bellettini,^{47b,47a} J. Bellinger,⁶⁰ D. Benjamin,¹⁷ A. Beretvas,¹⁸ A. Bhatti,⁵¹ M. Binkley,¹⁸ D. Bisello,^{44b,44a} I. Bizjak,^{31,dd} R. E. Blair,² C. Blocker,⁷ B. Blumenfeld,²⁶ A. Bocci,¹⁷ A. Bodek,⁵⁰ V. Boisvert,⁵⁰ D. Bortoletto,⁴⁹ J. Boudreau,⁴⁸ A. Boveia,¹¹ B. Brau,^{11,b} A. Bridgeman,²⁵ L. Brigliadori,^{6b,6a} C. Bromberg,³⁶ E. Brubaker,¹⁴ J. Budagov,¹⁶ H. S. Budd,⁵⁰ S. Budd,²⁵ K. Burkett,¹⁸ G. Busetto,^{44b,44a} P. Bussey,²² A. Buzatu,³⁴ K. L. Byrum,² S. Cabrera,^{17,y} C. Calancha,³² S. Camarda,⁴ M. Campanelli,³⁶ M. Campbell,³⁵ F. Canelli,^{14,18} A. Canepa,⁴⁶ B. Carls,²⁵ D. Carlsmith,⁶⁰ R. Carosi,^{47a} S. Carrillo,^{19,o} S. Carron,¹⁸ B. Casal,¹² M. Casarsa,¹⁸ A. Castro,^{6b,6a} P. Catastini,^{47c,47a} D. Cauz,^{55a} V. Cavaliere,^{47c,47a} M. Cavalli-Sforza,⁴ A. Cerri,²⁹ L. Cerrito,^{31,r} S. H. Chang,²⁸ Y. C. Chen,¹ M. Chertok,⁸ G. Chiarelli,^{47a} G. Chlachidze,¹⁸ F. Chlebana,¹⁸ K. Cho,²⁸ D. Chokheli,¹⁶ J. P. Chou,²³ G. Choudalakis,³³ K. Chung,^{18,p} W. H. Chung,⁶⁰ Y. S. Chung,⁵⁰ T. Chwalek,²⁷ C. I. Ciobanu,⁴⁵ M. A. Ciocci,^{47c,47a} A. Clark,²¹ D. Clark,⁷ G. Compostella,^{44a} M. E. Convery,¹⁸ J. Conway,⁸ M. Corbo,⁴⁵ M. Cordelli,²⁰ C. A. Cox,⁸ D. J. Cox,⁸ F. Crescioli,^{47b,47a} C. Cuenca Almenar,⁶¹ J. Cuevas,^{12,w} R. Culbertson,¹⁸ J. C. Cully,³⁵ D. Dagenhart,¹⁸ M. Datta,¹⁸ T. Davies,²² P. de Barbaro,⁵⁰ S. De Cecco,^{52a} A. Deisher,²⁹ G. De Lorenzo,⁴ M. Dell'Orso,^{47b,47a} C. Deluca,⁴ L. Demortier,⁵¹ J. Deng,^{17,g} M. Deninno,^{6a} M. d'Errico,^{44b,44a} A. Di Canto,^{47b,47a} G. P. di Giovanni,⁴⁵ B. Di Ruzza,^{47a} J. R. Dittmann,⁵ M. D'Onofrio,⁴ S. Donati,^{47b,47a} P. Dong,¹⁸ T. Dorigo,^{44a} S. Dube,⁵³ K. Ebina,⁵⁸ A. Elagin,⁵⁴ R. Erbacher,⁸ D. Errede,²⁵ S. Errede,²⁵ N. Ershaidat,^{45,cc} R. Eusebi,⁵⁴ H. C. Fang,²⁹ S. Farrington,⁴³ W. T. Fedorko,¹⁴ R. G. Feild,⁶¹ M. Feindt,²⁷ J. P. Fernandez,³² C. Ferrazza,^{47d,47a} R. Field,¹⁹ G. Flanagan,^{49,t} R. Forrest,⁸ M. J. Frank,⁵ M. Franklin,²³ J. C. Freeman,¹⁸ I. Furic,¹⁹ M. Gallinaro,⁵¹ J. Galyardt,¹³ F. Garberon,¹¹ J. E. Garcia,²¹ A. F. Garfinkel,⁴⁹ P. Garosi,^{47c,47a} K. Genser,¹⁸ H. Gerberich,²⁵ D. Gerdes,³⁵ A. Gessler,²⁷ S. Giagu,^{52b,52a} V. Giakoumopoulou,³ P. Giannetti,^{47a} K. Gibson,⁴⁸ J. L. Gimmell,⁵⁰ C. M. Ginsburg,¹⁸ N. Giokaris,³ M. Giordani,^{55b,55a} P. Giromini,²⁰ M. Giunta,^{47a} G. Giurgiu,²⁶ V. Glagolev,¹⁶ D. Glenzinski,¹⁸ M. Gold,³⁸ N. Goldschmidt,¹⁹ A. Golossanov,¹⁸ G. Gomez,¹² G. Gomez-Ceballos,³³ M. Goncharov,³³ O. González,³² I. Gorelov,³⁸ A. T. Goshaw,¹⁷ K. Goulianos,⁵¹ A. Gresele,^{44b,44a} S. Grinstein,⁴ C. Grosso-Pilcher,¹⁴ R. C. Group,¹⁸ U. Grundler,²⁵ J. Guimaraes da Costa,²³ Z. Gunay-Unalan,³⁶ C. Haber,²⁹ K. Hahn,³³ S. R. Hahn,¹⁸ E. Halkiadakis,⁵³ B.-Y. Han,⁵⁰ J. Y. Han,⁵⁰ F. Happacher,²⁰ K. Hara,⁵⁶ D. Hare,⁵³ M. Hare,⁵⁷ R. F. Harr,⁵⁹ M. Hartz,⁴⁸ K. Hatakeyama,⁵ C. Hays,⁴³ M. Heck,²⁷ J. Heinrich,⁴⁶ C. Henderson,³³ M. Herndon,⁶⁰ J. Heuser,²⁷ S. Hewamanage,⁵ D. Hidas,⁵³ C. S. Hill,^{11,d} D. Hirschbuehl,²⁷ A. Hocker,¹⁸ S. Hou,¹ M. Houlden,³⁰ S.-C. Hsu,²⁹ B. T. Huffman,⁴³ R. E. Hughes,⁴⁰ M. Hurwitz,¹⁴ U. Husemann,⁶¹ M. Hussein,³⁶ J. Huston,³⁶ J. Incandela,¹¹ G. Introzzi,^{47a} M. Iori,^{52b,52a} A. Ivanov,^{8,q} E. James,¹⁸ D. Jang,¹³ B. Jayatilaka,¹⁷ E. J. Jeon,²⁸ M. K. Jha,^{6a} S. Jindariani,¹⁸ W. Johnson,⁸ M. Jones,⁴⁹ K. K. Joo,²⁸ S. Y. Jun,¹³ J. E. Jung,²⁸ T. R. Junk,¹⁸ T. Kamon,⁵⁴ D. Kar,¹⁹ P. E. Karchin,⁵⁹ Y. Kato,^{42,n} R. Kephart,¹⁸ W. Ketchum,¹⁴ J. Keung,⁴⁶ V. Khotilovich,⁵⁴ B. Kilminster,¹⁸ D. H. Kim,²⁸ H. S. Kim,²⁸ H. W. Kim,²⁸ J. E. Kim,²⁸ M. J. Kim,²⁰ S. B. Kim,²⁸ S. H. Kim,⁵⁶ Y. K. Kim,¹⁴ N. Kimura,⁵⁸ L. Kirsch,⁷ S. Klimentenko,¹⁹ B. Knuteson,³³ K. Kondo,⁵⁸ D. J. Kong,²⁸ J. Konigsberg,¹⁹ A. Korytov,¹⁹ A. V. Kotwal,¹⁷ M. Krepis,²⁷ J. Kroll,⁴⁶ D. Krop,¹⁴ N. Krumnack,⁵ M. Kruse,¹⁷ V. Krutelyov,¹¹ T. Kuhr,²⁷ N. P. Kulkarni,⁵⁹ M. Kurata,⁵⁶ S. Kwang,¹⁴ A. T. Laasänen,⁴⁹ S. Lami,^{47a} S. Lammel,¹⁸ M. Lancaster,³¹ R. L. Lander,⁸ K. Lannon,^{40,v} A. Lath,⁵³ G. Latino,^{47c,47a} I. Lazzizzera,^{44b,44a} T. LeCompte,² E. Lee,⁵⁴ H. S. Lee,¹⁴ J. S. Lee,²⁸ S. W. Lee,^{54,x} S. Leone,^{47a} J. D. Lewis,¹⁸ C.-J. Lin,²⁹ J. Linacre,⁴³ M. Lindgren,¹⁸ E. Lipeles,⁴⁶ A. Lister,²¹ D. O. Litvintsev,¹⁸ C. Liu,⁴⁸ T. Liu,¹⁸ N. S. Lockyer,⁴⁶ A. Loginov,⁶¹ L. Lovas,¹⁵ D. Lucchesi,^{44b,44a} J. Lueck,²⁷ P. Lujan,²⁹ P. Lukens,¹⁸ G. Lungu,⁵¹ J. Lys,²⁹ R. Lysak,¹⁵ D. MacQueen,³⁴ R. Madrak,¹⁸ K. Maeshima,¹⁸ K. Makhoul,³³ P. Maksimovic,²⁶ S. Malde,⁴³ S. Malik,³¹ G. Manca,^{30,f} A. Manousakis-Katsikakis,³ F. Margaroli,⁴⁹ C. Marino,²⁷ C. P. Marino,²⁵ A. Martin,⁶¹ V. Martin,^{22,1} M. Martínez,⁴ R. Martínez-Ballarín,³² P. Mastrandrea,^{52a} M. Mathis,²⁶ M. E. Mattson,⁵⁹ P. Mazzanti,^{6a} K. S. McFarland,⁵⁰ P. McIntyre,⁵⁴ R. McNulty,^{30,k} A. Mehta,³⁰ P. Mehtala,²⁴ A. Menzione,^{47a} C. Mesropian,⁵¹ T. Miao,¹⁸ D. Miettlicki,³⁵ N. Miladinovic,⁷ R. Miller,³⁶ C. Mills,²³ M. Milnik,²⁷ A. Mitra,¹ G. Mitselmakher,¹⁹ H. Miyake,⁵⁶ S. Moed,²³ N. Moggi,^{6a} M. N. Mondragon,^{18,o} C. S. Moon,²⁸ R. Moore,¹⁸ M. J. Morello,^{47a} J. Morlock,²⁷ P. Movilla Fernandez,¹⁸ J. Müllenstädt,²⁹ A. Mukherjee,¹⁸ Th. Müller,²⁷ P. Murat,¹⁸ M. Mussini,^{6b,6a} J. Nachtman,^{18,p} Y. Nagai,⁵⁶ J. Naganoma,⁵⁶ K. Nakamura,⁵⁶ I. Nakano,⁴¹ A. Napier,⁵⁷ J. Nett,⁶⁰ C. Neu,^{46,aa} M. S. Neubauer,²⁵ S. Neubauer,²⁷ J. Nielsen,^{29,h} L. Nodulman,² M. Norman,¹⁰ O. Norriella,²⁵ E. Nurse,³¹ L. Oakes,⁴³ S. H. Oh,¹⁷ Y. D. Oh,²⁸ I. Oksuzian,¹⁹ T. Okusawa,⁴² R. Orava,²⁴ K. Osterberg,²⁴ S. Pagan Griso,^{44b,44a} C. Pagliarone,^{55a} E. Palencia,¹⁸ V. Papadimitriou,¹⁸ A. Papaikonomou,²⁷

A. A. Paramanov,² B. Parks,⁴⁰ S. Pashapour,³⁴ J. Patrick,¹⁸ G. Pauletta,^{55b,55a} M. Paulini,¹³ C. Paus,³³ T. Peiffer,²⁷ D. E. Pellett,⁸ A. Penzo,^{55a} T. J. Phillips,¹⁷ G. Piacentino,^{47a} E. Pianori,⁴⁶ L. Pinera,¹⁹ K. Pitts,²⁵ C. Plager,⁹ L. Pondrom,⁶⁰ K. Potamianos,⁴⁹ O. Poukhov,^{16,a} F. Prokoshin,^{16,z} A. Pronko,¹⁸ F. Ptohos,^{18,j} E. Pueschel,¹³ G. Punzi,^{47b,47a} J. Pursley,⁶⁰ J. Rademacker,^{43,d} A. Rahaman,⁴⁸ V. Ramakrishnan,⁶⁰ N. Ranjan,⁴⁹ I. Redondo,³² P. Renton,⁴³ M. Renz,²⁷ M. Rescigno,^{52a} S. Richter,²⁷ F. Rimondi,^{6b,6a} L. Ristori,^{47a} A. Robson,²² T. Rodrigo,¹² T. Rodriguez,⁴⁶ E. Rogers,²⁵ S. Rolli,⁵⁷ R. Roser,¹⁸ M. Rossi,^{55a} R. Rossin,¹¹ P. Roy,³⁴ A. Ruiz,¹² J. Russ,¹³ V. Rusu,¹⁸ B. Rutherford,¹⁸ H. Saarikko,²⁴ A. Safonov,⁵⁴ W. K. Sakumoto,⁵⁰ L. Santi,^{55b,55a} L. Sartori,^{47a} K. Sato,⁵⁶ A. Savoy-Navarro,⁴⁵ P. Schlabach,¹⁸ A. Schmidt,²⁷ E. E. Schmidt,¹⁸ M. A. Schmidt,¹⁴ M. P. Schmidt,^{61,a} M. Schmitt,³⁹ T. Schwarz,⁸ L. Scodellaro,¹² A. Scribano,^{47c,47a} F. Scuri,^{47a} A. Sedov,⁴⁹ S. Seidel,³⁸ Y. Seiya,⁴² A. Semenov,¹⁶ L. Sexton-Kennedy,¹⁸ F. Sforza,^{47b,47a} A. Sfyrila,²⁵ S. Z. Shalhout,⁵⁹ T. Shears,³⁰ P. F. Shepard,⁴⁸ M. Shimojima,^{56,u} S. Shiraishi,¹⁴ M. Shochet,¹⁴ Y. Shon,⁶⁰ I. Shreyber,³⁷ A. Simonenko,¹⁶ P. Sinervo,³⁴ A. Sisakyan,¹⁶ A. J. Slaughter,¹⁸ J. Slaunwhite,⁴⁰ K. Sliwa,⁵⁷ J. R. Smith,⁸ F. D. Snider,¹⁸ R. Snihur,³⁴ A. Soha,¹⁸ S. Somalwar,⁵³ V. Sorin,⁴ T. Spreitzer,³⁴ P. Squillacioti,^{47c,47a} M. Stanitzki,⁶¹ R. St. Denis,²² B. Stelzer,³⁴ O. Stelzer-Chilton,³⁴ D. Stentz,³⁹ J. Strologas,³⁸ G. L. Strycker,³⁵ J. S. Suh,²⁸ A. Sukhanov,¹⁹ I. Suslov,¹⁶ A. Taffard,^{25,g} R. Takashima,⁴¹ Y. Takeuchi,⁵⁶ R. Tanaka,⁴¹ J. Tang,¹⁴ M. Tecchio,³⁵ P. K. Teng,¹ J. Thom,^{18,i} J. Thome,¹³ G. A. Thompson,²⁵ E. Thomson,⁴⁶ P. Tipton,⁶¹ P. Ttito-Guzmán,³² S. Tkaczyk,¹⁸ D. Toback,⁵⁴ S. Tokar,¹⁵ K. Tollefson,³⁶ T. Tomura,⁵⁶ D. Tonelli,¹⁸ S. Torre,²⁰ D. Torretta,¹⁸ P. Totaro,^{55b,55a} S. Tournear,⁴⁵ M. Trovato,^{47d,47a} S.-Y. Tsai,¹ Y. Tu,⁴⁶ N. Turini,^{47c,47a} F. Ukegawa,⁵⁶ S. Uozumi,²⁸ N. van Remortel,^{24,c} A. Varganov,³⁵ E. Vataga,^{47d,47a} F. Vázquez,^{19,o} G. Velev,¹⁸ C. Vellidis,³ M. Vidal,³² I. Vila,¹² R. Vilar,¹² M. Vogel,³⁸ I. Volobouev,^{29,x} G. Volpi,^{47b,47a} P. Wagner,⁴⁶ R. G. Wagner,² R. L. Wagner,¹⁸ W. Wagner,^{27,bb} J. Wagner-Kuhr,²⁷ T. Wakisaka,⁴² R. Wallny,⁹ S. M. Wang,¹ A. Warburton,³⁴ D. Waters,³¹ M. Weinberger,⁵⁴ J. Weinelt,²⁷ W. C. Wester III,¹⁸ B. Whitehouse,⁵⁷ D. Whiteson,^{46,g} A. B. Wicklund,² E. Wicklund,¹⁸ S. Wilbur,¹⁴ G. Williams,³⁴ H. H. Williams,⁴⁶ P. Wilson,¹⁸ B. L. Winer,⁴⁰ P. Wittich,^{18,i} S. Wolbers,¹⁸ C. Wolfe,¹⁴ H. Wolfe,⁴⁰ T. Wright,³⁵ X. Wu,²¹ F. Würthwein,¹⁰ S. Xie,³³ A. Yagil,¹⁰ K. Yamamoto,⁴² J. Yamaoka,¹⁷ U. K. Yang,^{14,s} Y. C. Yang,²⁸ W. M. Yao,²⁹ G. P. Yeh,¹⁸ K. Yi,^{18,p} J. Yoh,¹⁸ K. Yorita,⁵⁸ T. Yoshida,^{42,m} G. B. Yu,¹⁷ I. Yu,²⁸ S. S. Yu,¹⁸ J. C. Yun,¹⁸ A. Zanetti,^{55a} Y. Zeng,¹⁷ X. Zhang,²⁵ Y. Zheng,^{9,e} and S. Zucchelli^{6b,6a}

(CDF Collaboration)

¹*Institute of Physics, Academia Sinica, Taipei, Taiwan 11529, Republic of China*²*Argonne National Laboratory, Argonne, Illinois 60439, USA*³*University of Athens, 157 71 Athens, Greece*⁴*Institut de Física d'Altes Energies, Universitat Autònoma de Barcelona, E-08193, Bellaterra (Barcelona), Spain*⁵*Baylor University, Waco, Texas 76798, USA*^{6a}*Istituto Nazionale di Fisica Nucleare Bologna, I-40127 Bologna, Italy*^{6b}*University of Bologna, I-40127 Bologna, Italy*⁷*Brandeis University, Waltham, Massachusetts 02254, USA*⁸*University of California, Davis, Davis, California 95616, USA*⁹*University of California, Los Angeles, Los Angeles, California 90024, USA*¹⁰*University of California, San Diego, La Jolla, California 92093, USA*¹¹*University of California, Santa Barbara, Santa Barbara, California 93106, USA*¹²*Instituto de Física de Cantabria, CSIC-University of Cantabria, 39005 Santander, Spain*¹³*Carnegie Mellon University, Pittsburgh, Pennsylvania 15213, USA*¹⁴*Enrico Fermi Institute, University of Chicago, Chicago, Illinois 60637, USA*¹⁵*Comenius University, 842 48 Bratislava, Slovakia; Institute of Experimental Physics, 040 01 Kosice, Slovakia*¹⁶*Joint Institute for Nuclear Research, RU-141980 Dubna, Russia*¹⁷*Duke University, Durham, North Carolina 27708, USA*¹⁸*Fermi National Accelerator Laboratory, Batavia, Illinois 60510, USA*¹⁹*University of Florida, Gainesville, Florida 32611, USA*²⁰*Laboratori Nazionali di Frascati, Istituto Nazionale di Fisica Nucleare, I-00044 Frascati, Italy*²¹*University of Geneva, CH-1211 Geneva 4, Switzerland*²²*Glasgow University, Glasgow G12 8QQ, United Kingdom*²³*Harvard University, Cambridge, Massachusetts 02138, USA*²⁴*Division of High Energy Physics, Department of Physics, University of Helsinki and Helsinki Institute of Physics, FIN-00014, Helsinki, Finland*²⁵*University of Illinois, Urbana, Illinois 61801, USA*²⁶*The Johns Hopkins University, Baltimore, Maryland 21218, USA*²⁷*Institut für Experimentelle Kernphysik, Karlsruhe Institute of Technology, D-76131 Karlsruhe, Germany*

- ²⁸*Center for High Energy Physics: Kyungpook National University, Daegu 702-701, Korea; Seoul National University, Seoul 151-742, Korea; Sungkyunkwan University, Suwon 440-746, Korea; Korea Institute of Science and Technology Information, Daejeon 305-806, Korea; Chonnam National University, Gwangju 500-757, Korea; Chonbuk National University, Jeonju 561-756, Korea*
- ²⁹*Ernest Orlando Lawrence Berkeley National Laboratory, Berkeley, California 94720, USA*
- ³⁰*University of Liverpool, Liverpool L69 7ZE, United Kingdom*
- ³¹*University College London, London WC1E 6BT, United Kingdom*
- ³²*Centro de Investigaciones Energeticas, Medioambientales y Tecnologicas, E-28040 Madrid, Spain*
- ³³*Massachusetts Institute of Technology, Cambridge, Massachusetts 02139, USA*
- ³⁴*Institute of Particle Physics: McGill University, Montréal, Québec, Canada H3A 2T8; Simon Fraser University, Burnaby, British Columbia, Canada V5A 1S6; University of Toronto, Toronto, Ontario, Canada M5S 1A7; and TRIUMF, Vancouver, British Columbia, Canada V6T 2A3*
- ³⁵*University of Michigan, Ann Arbor, Michigan 48109, USA*
- ³⁶*Michigan State University, East Lansing, Michigan 48824, USA*
- ³⁷*Institution for Theoretical and Experimental Physics, ITEP, Moscow 117259, Russia*
- ³⁸*University of New Mexico, Albuquerque, New Mexico 87131, USA*
- ³⁹*Northwestern University, Evanston, Illinois 60208, USA*
- ⁴⁰*The Ohio State University, Columbus, Ohio 43210, USA*
- ⁴¹*Okayama University, Okayama 700-8530, Japan*
- ⁴²*Osaka City University, Osaka 588, Japan*
- ⁴³*University of Oxford, Oxford OX1 3RH, United Kingdom*
- ^{44a}*Istituto Nazionale di Fisica Nucleare, Sezione di Padova-Trento, I-35131 Padova, Italy*
- ^{44b}*University of Padova, I-35131 Padova, Italy*
- ⁴⁵*LPNHE, Universite Pierre et Marie Curie/IN2P3-CNRS, UMR7585, Paris, F-75252 France*
- ⁴⁶*University of Pennsylvania, Philadelphia, Pennsylvania 19104, USA*
- ^{47a}*Istituto Nazionale di Fisica Nucleare Pisa, I-56127 Pisa, Italy*
- ^{47b}*University of Pisa, I-56127 Pisa, Italy*
- ^{47c}*University of Siena, I-56127 Pisa, Italy*
- ^{47d}*Scuola Normale Superiore, I-56127 Pisa, Italy*
- ⁴⁸*University of Pittsburgh, Pittsburgh, Pennsylvania 15260, USA*
- ⁴⁹*Purdue University, West Lafayette, Indiana 47907, USA*
- ⁵⁰*University of Rochester, Rochester, New York 14627, USA*
- ⁵¹*The Rockefeller University, New York, New York 10021, USA*
- ^{52a}*Istituto Nazionale di Fisica Nucleare, Sezione di Roma 1, I-00185 Roma, Italy*

^aDeceased.

^bVisitor from University of Massachusetts Amherst, Amherst, MA 01003, USA.

^cVisitor from Universiteit Antwerpen, B-2610 Antwerp, Belgium.

^dVisitor from University of Bristol, Bristol BS8 1TL, United Kingdom.

^eVisitor from Chinese Academy of Sciences, Beijing 100864, China.

^fVisitor from Istituto Nazionale di Fisica Nucleare, Sezione di Cagliari, 09042 Monserrato (Cagliari), Italy.

^gVisitor from University of California Irvine, Irvine, CA 92697, USA.

^hVisitor from University of California Santa Cruz, Santa Cruz, CA 95064, USA.

ⁱVisitor from Cornell University, Ithaca, NY 14853, USA.

^jVisitor from University of Cyprus, Nicosia CY-1678, Cyprus.

^kVisitor from University College Dublin, Dublin 4, Ireland.

^lVisitor from University of Edinburgh, Edinburgh EH9 3JZ, United Kingdom.

^mVisitor from University of Fukui, Fukui City, Fukui Prefecture, Japan 910-0017.

ⁿVisitor from Kinki University, Higashi-Osaka City, Japan 577-8502.

^oVisitor from Universidad Iberoamericana, Mexico D.F., Mexico.

^pVisitor from University of Iowa, Iowa City, IA 52242, USA.

^qVisitor from Kansas State University, Manhattan, KS 66506, USA.

^rVisitor from Queen Mary, University of London, London, E1 4NS, United Kingdom.

^sVisitor from University of Manchester, Manchester M13 9PL, United Kingdom.

^tVisitor from Muons, Inc., Batavia, IL 60510, USA.

^uVisitor from Nagasaki Institute of Applied Science, Nagasaki, Japan.

^wVisitor from University de Oviedo, E-33007 Oviedo, Spain.

^xVisitor from Texas Tech University, Lubbock, TX 79609, USA.

^yVisitor from IFIC (CSIC-Universitat de Valencia), 56071 Valencia, Spain.

^zVisitor from Universidad Tecnica Federico Santa Maria, 110V Valparaiso, Chile.

^{aa}Visitor from University of Virginia, Charlottesville, VA 22906, USA.

^{bb}Visitor from Bergische Universität Wuppertal, 42097 Wuppertal, Germany.

^{cc}Visitor from Yarmouk University, Irbid 211-63, Jordan.

^{dd}On leave from J. Stefan Institute, Ljubljana, Slovenia.

^{52b}*Sapienza Università di Roma, I-00185 Roma, Italy*⁵³*Rutgers University, Piscataway, New Jersey 08855, USA*⁵⁴*Texas A&M University, College Station, Texas 77843, USA*^{55a}*Istituto Nazionale di Fisica Nucleare Trieste/Udine, I-34100 Trieste, I-33100 Udine, Italy*^{55b}*University of Trieste/Udine, I-33100 Udine, Italy*⁵⁶*University of Tsukuba, Tsukuba, Ibaraki 305, Japan*⁵⁷*Tufts University, Medford, Massachusetts 02155, USA*⁵⁸*Waseda University, Tokyo 169, Japan*⁵⁹*Wayne State University, Detroit, Michigan 48201, USA*⁶⁰*University of Wisconsin, Madison, Wisconsin 53706, USA*⁶¹*Yale University, New Haven, Connecticut 06520, USA*

(Received 17 November 2009; published 16 February 2010)

We present measurements of the top quark mass using m_{T2} , a variable related to the transverse mass in events with two missing particles. We use the template method applied to $t\bar{t}$ dilepton events produced in $p\bar{p}$ collisions at Fermilab's Tevatron Collider and collected by the CDF detector. From a data sample corresponding to an integrated luminosity of 3.4 fb^{-1} , we select 236 $t\bar{t}$ candidate events. Using the m_{T2} distribution, we measure the top quark mass to be $M_{\text{top}} = 168.0_{-4.0}^{+4.8}(\text{stat}) \pm 2.9(\text{syst}) \text{ GeV}/c^2$. By combining m_{T2} with the reconstructed top quark mass distributions based on a neutrino weighting method, we measure $M_{\text{top}} = 169.3 \pm 2.7(\text{stat}) \pm 3.2(\text{syst}) \text{ GeV}/c^2$. This is the first application of the m_{T2} variable in a mass measurement at a hadron collider.

DOI: [10.1103/PhysRevD.81.031102](https://doi.org/10.1103/PhysRevD.81.031102)

PACS numbers: 14.65.Ha, 12.15.Ff, 13.85.Ni, 13.85.Qk

I. INTRODUCTION

Models in numerous, well-motivated theoretical frameworks make predictions for new phenomena at hadron colliders such as the Tevatron and the Large Hadron Collider (LHC) [1,2]. Within each framework, one can construct a number of qualitatively different models consistent with data. Thus, when discoveries are made at a hadron collider, we face the inverse problem of how one maps back to the underlying theory responsible for the new phenomena [1,3]. A potentially powerful observable to discriminate among models and to extract the mass of new particles, when the new phenomenon produces a pair of new particles with large missing energy signatures, is the m_{T2} variable [4,5]. The m_{T2} variable is based on transverse mass in events with two missing particles.

The top quark is the heaviest known elementary particle with a mass approximately 40 times larger than the mass of its isospin partner, the bottom quark (b). The large top quark mass (M_{top}) produces significant contributions to electroweak radiative corrections. Therefore, top quark mass measurements are important tests of the standard model and provide constraints on the Higgs boson mass. In the dilepton channel, $t\bar{t}$ pair production is followed by the decay of each top quark to a W boson and a b quark where both W bosons then decay to charged leptons (e or μ) and neutrinos. Events in this channel thus contain two leptons, two b quark jets, and two undetected neutrinos. The measurement of M_{top} using complementary techniques tests and improves our understanding of this important parameter in the standard model [6].

In this paper, we present the first measurement of the mass of the top quark using the m_{T2} distribution with $t\bar{t}$

events in the dilepton channel [7]. We use this channel because it has decay products similar to possible new phenomena where undetected particles are created. We compare this method with two others that were previously used: the reconstructed top quark mass using the neutrino weighting algorithm (m_t^{NWA}) [8,9] and the scalar sum of transverse energies of jets, leptons, and missing transverse energy (\cancel{E}_T) [10] in the event (H_T) [11]. We also measure the top quark mass using pairs of observables [$(m_{T2}, m_t^{\text{NWA}})$ and (m_t^{NWA}, H_T)] simultaneously.

II. THE m_{T2} VARIABLE

Many models contain heavy, strongly interacting particles with the same conserved charge or parity that result in weakly interacting, stable particles in the final state. A hadron collider would pair produce these colored particles, which then decay into standard model particles along with a pair of undetectable weakly interacting particles, so that the generic experimental signature is large missing transverse momentum accompanied by multiple energetic jets and leptons [10]. In this final state, we can define m_{T2} as

$$m_{T2}(m_{\text{invis}}) = \min_{\mathbf{p}_T^{(1)}, \mathbf{p}_T^{(2)}} [\max[m_T(m_{\text{invis}}; \mathbf{p}_T^{(1)}), m_T(m_{\text{invis}}; \mathbf{p}_T^{(2)})]], \quad (1)$$

where m_T , the transverse mass of each parent particle, is defined as

$$m_T(m_{\text{invis}}; \mathbf{p}_T^{\text{invis}}) = \sqrt{m_{\text{vis}}^2 + m_{\text{invis}}^2 + 2(E_T^{\text{vis}} E_T^{\text{invis}} - \mathbf{p}_T^{\text{vis}} \cdot \mathbf{p}_T^{\text{invis}})}. \quad (2)$$

Here “invis” and “vis” represent the individual unde-

ected (invisible) and detected (visible) particles, respectively, $\mathbf{p}_T^{(1)}$ and $\mathbf{p}_T^{(2)}$ are transverse momenta of two invisible particles, and m_{invis} is the mass of the invisible particle. The minimization is performed with the constraint $\mathbf{p}_T^{(1)} + \mathbf{p}_T^{(2)} = \mathbf{p}_T^{\text{missing}}$, where the magnitude of $\mathbf{p}_T^{\text{missing}}$ is constrained to the missing transverse momentum.

The quantity m_{T2} represents a lower bound on the mass of the parent particle. Using the m_{T2} distribution, we can extract the mass of this parent particle [12] in a similar way to the precise measurement of the W boson mass [13] where an event contains one charged lepton (e or μ) and a neutrino, with the latter not being detected.

III. EXPERIMENT AND DATA

We use a sample of $t\bar{t}$ candidates in the dilepton channel, corresponding to 3.4 fb^{-1} of proton-antiproton collisions at $\sqrt{s} = 1.96 \text{ TeV}$, collected using the CDF II detector [14]. This is a general-purpose detector designed to study $p\bar{p}$ collisions at the Fermilab Tevatron. A charged-particle tracking system, consisting of a silicon microstrip tracker and a drift chamber, is immersed in a 1.4 T magnetic field. Electromagnetic and hadronic calorimeters surround the tracking system and measure particle energies. Drift chambers and scintillators, located outside the calorimeters, detect muon candidates.

We select events consistent with the $t\bar{t}$ dilepton decay topology. We require two oppositely charged lepton candidates with $p_T > 20 \text{ GeV}/c$ with one isolated [15] lepton candidate in the central region ($|\eta| < 1$) of the detector, and another isolated or nonisolated lepton candidate in the central region, or isolated electron candidate in the forward region ($1.0 < |\eta| < 2.0$). We also require \cancel{E}_T exceeding 25 GeV , and at least two jets with $E_T > 15 \text{ GeV}$ and $|\eta| < 2.5$ [10]. To further reject backgrounds, we request $H_T > 200 \text{ GeV}$. We also require the variables of interest to be consistent with the top quark hypothesis by demanding $20 \text{ GeV}/c^2 < m_{T2} < 300 \text{ GeV}/c^2$ and $100 \text{ GeV}/c^2 < m_i^{\text{NWA}} < 350 \text{ GeV}/c^2$. The criteria select 236 $t\bar{t}$ candidate events.

The primary sources of background production are Drell-Yan, diboson, and QCD multijet events. We estimate the rate of the Drell-Yan events with a calculation based on simulated events using the ALPGEN [16] v2.10 Monte Carlo (MC) generator and the rate of diboson events with a PYTHIA [17] v6.216 calculation. For the Drell-Yan Z + jets process, we normalize the MC sample by matching the number of Z events predicted and observed in the Z mass region between 76 and $106 \text{ GeV}/c^2$. We use data to estimate the rate of background events from QCD multijet production where an event has one real lepton and one of the jets misidentified as another lepton (fake). In measuring the top quark mass, we divide the $t\bar{t}$ candidate sample into events with and without secondary vertex b tags [18], which have very different purity. We only attempt to b

TABLE I. Expected and observed numbers of signal and background events assuming $t\bar{t}$ production cross section $\sigma_{t\bar{t}} = 6.7 \pm 0.8 \text{ pb}$ and $M_{\text{top}} = 175 \text{ GeV}/c^2$. Uncertainties quoted capture the uncertainties on the theoretical cross section, the statistics of data in the Z mass window, the jet energy scale, the luminosity, the fake rates, and the statistics of the MC samples.

	Nontagged	Tagged
Diboson	15.2 ± 2.3	0.6 ± 0.1
Drell-Yan	31.1 ± 3.5	1.7 ± 0.2
QCD multijets	31.2 ± 8.7	4.5 ± 1.3
Total background	77.5 ± 9.8	6.8 ± 1.3
$t\bar{t}$ with $\sigma_{t\bar{t}} = 6.7 \text{ pb}$	68.7 ± 6.8	88.4 ± 8.2
Total (predicted)	146.2 ± 11.9	95.2 ± 8.3
Observed (3.4 fb^{-1})	149	87

tag the two highest E_T jets. Table I summarizes the composition of background events and the expected numbers of $t\bar{t}$ and background events. We estimate the $t\bar{t}$ signal event rates using PYTHIA v6.216 with CTEQSL [19] parton distribution functions at leading order with a full detector simulation [20].

To calculate m_{T2} of a $t\bar{t}$ dilepton event [7], we first identify all possible configurations corresponding to different assignments of jets to b quarks and combinations of quarks and leptons. The two most energetic jets in an event are considered to have originated from the b quarks. For each configuration, we calculate the transverse mass of each top quark ($t \rightarrow b l \nu$) using Eq. (2):

$$m_T = \sqrt{m_{bl}^2 + m_\nu^2 + 2(E_T^{bl} E_T^\nu - \mathbf{p}_T^{bl} \cdot \mathbf{p}_T^\nu)}, \quad (3)$$

where m_{bl} and \mathbf{p}_T^{bl} denote the invariant mass and transverse momentum of the bottom-quark jets and charged lepton (bl) system, m_ν and \mathbf{p}_T^ν are the mass and transverse momentum of the neutrino, and E_T^{bl} and E_T^ν are the transverse energies of the bl system and neutrino:

$$E_T^{bl} = \sqrt{|\mathbf{p}_T^{bl}|^2 + m_{bl}^2} \quad \text{and} \quad E_T^\nu = \sqrt{|\mathbf{p}_T^\nu|^2 + m_\nu^2}. \quad (4)$$

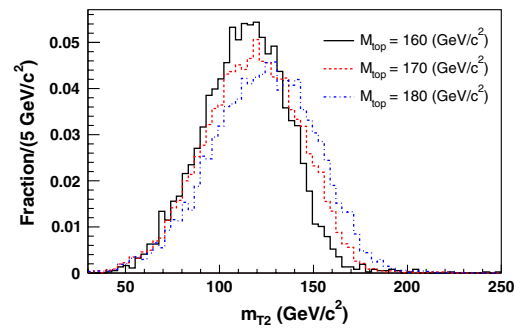


FIG. 1 (color online). The m_{T2} distributions from $t\bar{t}$ dilepton Monte Carlo events that pass the selection criteria for three input values of the top quark mass. Each distribution is normalized to have unit area.

We then calculate m_{T2} using Eq. (1) with the assumption $m_\nu = 0$, and for all possible parton assignments. We select the smallest value for each event. Figure 1 shows simulated m_{T2} distributions for various top quark masses for the combined non- b -tagged and b -tagged sample, which demonstrates that m_{T2} is sensitive to M_{top} , and thus can be used to measure it.

IV. MASS FIT

We estimate the probability density functions (PDFs) of signals and background using the kernel density estimation (KDE) [21,22] that constructs the PDF without any assumption of a functional form. For the mass measurement with two observables, we use the two-dimensional KDE that accounts for the correlation between the two observables. First, at discrete values of M_{top} from 130 to 220 GeV/c^2 with increments of 0.5 GeV/c^2 in the region immediately above and below 175 to 5 GeV/c^2 near the extreme mass values, we estimate the PDFs for the observables from 76 $t\bar{t}$ MC samples. Each sample consists of 0.6 to 4.8 M generated events, with 1 M events corresponding to a luminosity of 150 fb^{-1} , assuming a $t\bar{t}$ cross section of 6.7 pb [23]. We smooth and interpolate the MC distributions to find PDFs for arbitrary values of M_{top} using the local polynomial smoothing method [24]. We fit the distributions of the observables in the data to the signal and background PDFs in an unbinned extended maximum likelihood fit [25], where we minimize the negative logarithm of the likelihood using MINUIT [26]. The likelihood is built for the b -tagged and non- b -tagged categories separately and then combined by multiplying the two categories. We find the statistical uncertainty on M_{top} by searching for the points where the negative logarithm of the likelihood minimized with respect to all other parameters deviates by 0.5 units from the minimum. Reference [22] provides detailed information about this technique.

We test the mass fit procedures using 3000 pseudoexperiments for each of 14 different top quark masses ranging from 159 to 185 GeV/c^2 with almost 2 GeV/c^2 step size. In each experiment, we select the numbers of background events from a Poisson distribution with a mean equal to the expected numbers of background events in the sample and the numbers of signal events from a Poisson distribution with a mean equal to the expected numbers of signal events assuming a $t\bar{t}$ pair production cross section of 6.7 pb. The distributions of the average mass residual (deviation from the input top mass) and the width of the pull (the ratio of the residual to the uncertainty reported by MINUIT) for simulated experiments show that the measured top quark mass is on average $0.26 \pm 0.10 \text{ GeV}/c^2$ lower than the true top quark mass and has no dependence on M_{top} in the m_{T2} measurements. We correct the measurement for this bias. No such bias is observed with the

combined (m_{T2}, m_i^{NWA}) measurement. In all cases, the fit on average correctly estimates the statistical uncertainties, based on the pull width distribution being consistent with unity. For $M_{\text{top}} = 175 \text{ GeV}/c^2$, we expect the statistical uncertainties on M_{top} to be 4.0 GeV/c^2 with m_{T2} , 3.4 GeV/c^2 with m_i^{NWA} , 5.4 GeV/c^2 with H_T , 2.9 GeV/c^2 with $(m_{T2}, m_i^{\text{NWA}})$ combined, and 3.2 GeV/c^2 with (m_i^{NWA}, H_T) combined.

V. SYSTEMATIC UNCERTAINTIES

We examine a variety of systematic effects that could affect the measurement by comparing MC simulated experiments in which we vary relevant parameters within their systematic uncertainties. The dominant source of systematic uncertainty is the light quark jet energy scale (JES) [27]. We vary JES parameters within their uncertainties in both signal and background MC generated events and interpret the shifts as uncertainties. The b -jet energy scale systematic uncertainty arising from our modeling of b fragmentation, b hadron branching fractions, and calorimeter response captures the additional uncertainty not taken into account in the light quark jet energy scale. The uncertainty arising from the choice of MC generator is estimated by comparing MC simulated experiments generated with PYTHIA and HERWIG [28]. We estimate the systematic uncertainty due to modeling of initial-state gluon radiation and final-state gluon radiation by extrapolating uncertainties in the p_T of Drell-Yan events to the $t\bar{t}$ mass region [29]. We estimate the systematic uncertainty due to parton distribution functions by varying the independent eigenvectors of the CTEQ6M [30] parton distribution functions, varying Λ_{QCD} , and comparing CTEQ5L [19] with MRST72 [31] parton distribution functions. In estimating the systematic uncertainty associated with uncertainties in the top quark production mechanism, we vary the fraction of top quarks produced by gluon-gluon annihilation from 6% to 20%, corresponding to the 1 standard deviation upper bound on the gluon fusion fraction [32]. We estimate systematic uncertainties due to the lepton energy and momentum scales by propagating shifts in electron energy and muon momentum scales within their uncertainties. Background shape systematic uncertainties account for the variation of the background composition. In addition, we change the shape of the Drell-Yan background sample according to the difference in the missing energy distribution observed in data and simulation, and the shape of the QCD multijet model. We estimate the multiple hadron interaction systematic uncertainties to account for the fact that the average number of interactions in our MC samples are not equal to the number observed in the data. We extract the mass dependence on the number of interactions in MC pseudoexperiments by dividing our MC samples into subsamples with different number of inter-

actions. We then multiply the slope of the result by the difference in the number of interactions between MC events and data and treat that as a systematic uncertainty.

It has been suggested that color reconnection (CR) effects could cause a bias in the top quark mass measurement and interpretations at the level of $0.5 \text{ GeV}/c^2$ [33]. We estimate uncertainties arising from CR effects using the PYTHIA 6.4 MC generator, which includes CR effects and other new features in modeling the underlying event, initial and final-state radiation, and parton showering. We generate two MC samples, one using tune A [34], which is very similar to the tune for CDF nominal MC generations, the other using A_{CR} [33], which includes CR into the tune A. We take the difference in the extracted mass between these two MC samples as a systematic uncertainty. We measure the difference to be 0.6 GeV for $(m_{T2}, m_i^{\text{NWA}})$ combined, and 0.7 GeV for m_{T2} alone. As a cross-check, we generate two other MC samples, one using tune S_0 [33] and the other using NOCR [33], which include all of the new features with and without CR. We find a similar mass difference between the two samples.

Table II summarizes the sources and estimates of systematic uncertainties. The total systematic uncertainties, adding them in quadrature, are $2.9 \text{ GeV}/c^2$ with m_{T2} , $3.8 \text{ GeV}/c^2$ with m_i^{NWA} , $5.7 \text{ GeV}/c^2$ with H_T , $3.2 \text{ GeV}/c^2$ with $(m_{T2}, m_i^{\text{NWA}})$ combined, and $3.8 \text{ GeV}/c^2$ with (m_i^{NWA}, H_T) combined. The m_{T2} method has a jet energy scale uncertainty significantly smaller than m_i^{NWA} , resulting in the smallest total systematic uncertainty. Including both statistical and systematic uncertainties, we conclude that m_{T2} is one of the best observables for the M_{top} measurement, comparable to the measurement using m_i^{NWA} . Using both m_{T2} and m_i^{NWA} , we expect to achieve a 10% improvement in overall uncertainty over using m_{T2} alone.

VI. RESULTS

We apply a likelihood fit to the data using observables discussed in this article. Figure 2 shows the one-dimensional log-likelihoods for m_{T2} and $(m_{T2}, m_i^{\text{NWA}})$ combined. Figure 3 shows the distributions of the observables used for the M_{top} measurements overlaid with density estimates using $t\bar{t}$ signal events with $M_{\text{top}} = 169 \text{ GeV}/c^2$ and the full background model. The fit results are summarized in Table III. The extracted masses are consistent with each other and the statistical uncertainties are consistent with predictions from MC pseudoexperiments.

In conclusion, we present the top quark mass measurements in the dilepton channel using m_{T2} . In 3.4 fb^{-1} of CDF data, we measure M_{top} using m_{T2} to be

$$\begin{aligned} M_{\text{top}} &= 168.0_{-4.0}^{+4.8}(\text{stat}) \pm 2.9(\text{syst}) \text{ GeV}/c^2 \\ &= 168.0_{-5.0}^{+5.6} \text{ GeV}/c^2, \end{aligned}$$

and using both m_i^{NWA} and m_{T2} to be

$$\begin{aligned} M_{\text{top}} &= 169.3 \pm 2.7(\text{stat}) \pm 3.2(\text{syst}) \text{ GeV}/c^2 \\ &= 169.3 \pm 4.2 \text{ GeV}/c^2. \end{aligned}$$

This is consistent with the most precise published result in this channel from the CDF [35] and D0 [36] Collaborations. We expect further improvements in M_{top} with these variables as CDF accumulates about a factor of 3 more data during Tevatron run II. The measurements in this article are the first application of the m_{T2} variable to data, and demonstrate that m_{T2} is a powerful observable for the mass measurement of the top quark in the dilepton channel. The methods described in this article will be applicable to other measurements at the Tevatron and soon at CERN's Large Hadron Collider for discriminating new physics models and measuring the mass of heavy

TABLE II. Estimated statistical ($M_{\text{top}} = 175 \text{ GeV}/c^2$), systematic, and total uncertainties in GeV/c^2 .

		m_{T2}	m_i^{NWA}	H_T	$(m_i^{\text{NWA}}, m_{T2})$	(m_i^{NWA}, H_T)
Statistical		4.0	3.4	5.4	2.9	3.2
Systematic	Jet energy scale (light quarks)	2.6	3.5	3.7	3.0	3.4
	Generator	0.3	1.0	2.6	0.5	1.3
	Parton distribution functions	0.5	0.6	1.8	0.5	0.8
	b jet energy scale	0.2	0.3	0.2	0.2	0.3
	Background shape	0.4	0.3	0.7	0.1	0.3
	Gluon fusion fraction	0.3	0.1	0.3	<0.1	0.1
	Initial- and final-state radiation	0.6	0.2	0.6	0.3	0.2
	MC statistics	0.3	0.3	0.5	0.3	0.3
	Lepton energy	0.6	0.2	0.7	0.3	0.2
	Multiple hadron interaction	0.2	0.3	0.3	0.3	0.3
	Color reconnection	0.7	0.6	2.5	0.6	0.6
Total systematic uncertainty		2.9	3.8	5.7	3.2	3.8
Total		5.0	5.1	7.8	4.3	5.0

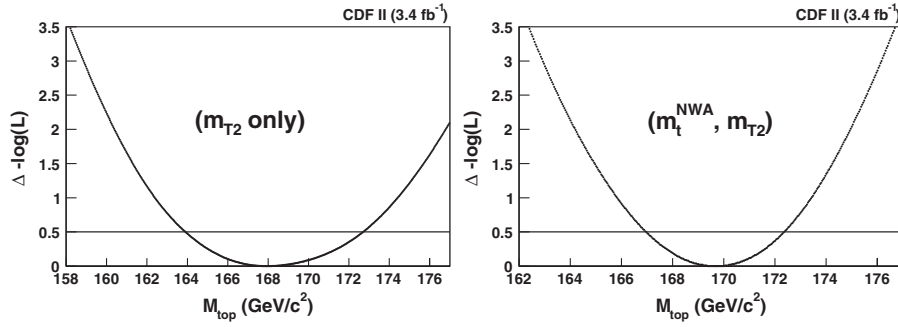
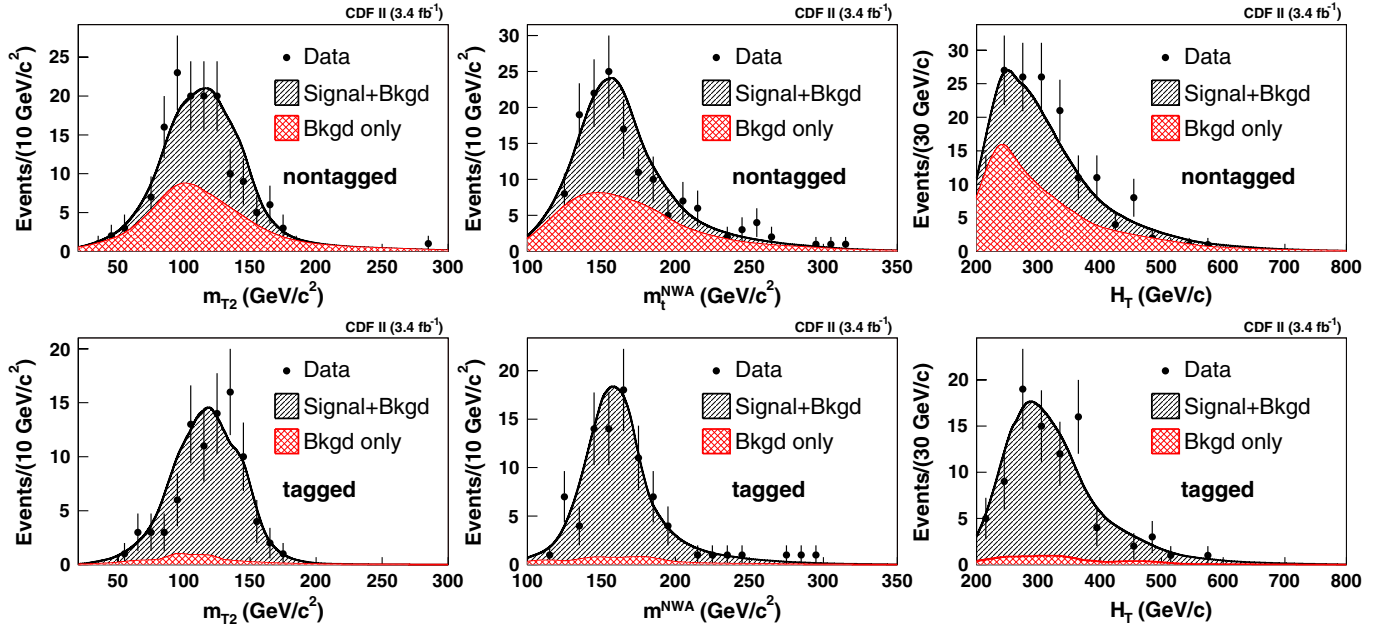


FIG. 2. Negative log-likelihood distributions.

FIG. 3 (color online). Distributions of the three variables used to estimate the top quark mass, showing the b -tagged and non- b -tagged samples separately. The data are overlaid with the predictions from the KDE probability distributions using the top quark mass $M_{\text{top}} = 169 \text{ GeV}/c^2$ and full background model.

particles that decay into weakly interacting particles such as dark matter candidates.

ACKNOWLEDGMENTS

We thank the Fermilab staff and the technical staffs of the participating institutions for their vital contributions.

TABLE III. Summary of top quark mass measurements with different observables. In the right-hand M_{top} column, we combine in quadrature the statistical and systematic uncertainty in order to compare the precision of the different methods.

Observables	M_{top} (GeV/ c^2)	M_{top} (GeV/ c^2)
m_{T_2}	$168.0^{+4.8}_{-4.0}(\text{stat}) \pm 2.9(\text{syst})$	$168.0^{+5.6}_{-5.0}$
m_t^{NWA}	$169.4^{+3.3}_{-3.2}(\text{stat}) \pm 3.8(\text{syst})$	$169.4^{+5.0}_{-5.0}$
H_T	$168.8^{+5.1}_{-6.6}(\text{stat}) \pm 5.7(\text{syst})$	$168.8^{+7.6}_{-8.7}$
m_t^{NWA} and m_{T_2}	$169.3^{+2.7}_{-2.7}(\text{stat}) \pm 3.2(\text{syst})$	$169.3^{+4.2}_{-4.2}$
m_t^{NWA} and H_T	$169.6^{+2.8}_{-2.9}(\text{stat}) \pm 3.8(\text{syst})$	$169.6^{+4.7}_{-4.8}$

This work was supported by the U.S. Department of Energy and the National Science Foundation; the Italian Istituto Nazionale di Fisica Nucleare; the Ministry of Education, Culture, Sports, Science and Technology of Japan; the Natural Sciences and Engineering Research Council of Canada; the National Science Council of the Republic of China; the Swiss National Science Foundation; the A. P. Sloan Foundation; the Bundesministerium für Bildung und Forschung, Germany; the Korean Science and Engineering Foundation and the Korean Research Foundation; the Science and Technology Facilities Council and the Royal Society, UK; the Institut National de Physique Nucleaire et Physique des Particules/CNRS; the Russian Foundation for Basic Research; the Ministerio de Ciencia e Innovación, and the Programa Consolider-Ingenio 2010, Spain; the Slovak R&D Agency; and the Academy of Finland.

- [1] S. Abdullin *et al.* (TeV4LHC Working Group), arXiv:hep-ph/0608322v2.
- [2] G. Brooijmans *et al.*, arXiv:0802.3715v1.
- [3] A. K. Datta, K. Kong, and K. T. Matchev, Phys. Rev. D **72**, 096006 (2005).
- [4] C. Lester and D. Summers, Phys. Lett. B **463**, 99 (1999).
- [5] A. Barr, C. Lester, and P. Stephens, J. Phys. G **29**, 2343 (2003).
- [6] C. Amsler *et al.* (Particle Data Group), Phys. Lett. B **667**, 1 (2008).
- [7] W. S. Cho, K. Choi, Y. G. Kim, and C. B. Park, Phys. Rev. D **78**, 034019 (2008).
- [8] B. Abbott *et al.* (D0 Collaboration), Phys. Rev. D **60**, 052001 (1999).
- [9] A. Abulencia *et al.* (CDF Collaboration), Phys. Rev. D **73**, 112006 (2006).
- [10] We use a right-handed cylindrical coordinate system with the origin in the center of the detector, where θ and ϕ are the polar and azimuthal angles and pseudorapidity is defined as $\eta = -\text{Intan}(\theta/2)$. Transverse energy and momentum are $E_T = E \sin(\theta)$ and $p_T = p \sin(\theta)$, respectively, where E and p are energy and momentum. Undetected particles, such as neutrinos from leptonic W decays, lead to an imbalance of energy (momentum) in the transverse plane of the detector, \cancel{E}_T (p_T^{missing}).
- [11] F. Abe *et al.* (CDF Collaboration), Phys. Rev. Lett. **75**, 3997 (1995).
- [12] M. Burns, K. Kong, K. T. Matchev, and M. Park, J. High Energy Phys. 03 (2009) 143.
- [13] A. Abulencia *et al.* (CDF Collaboration), Phys. Rev. Lett. **99**, 151801 (2007).
- [14] D. Acosta *et al.* (CDF Collaboration), Phys. Rev. D **71**, 032001 (2005).
- [15] A lepton is isolated if the total E_T (p_T) within a cone with $\Delta R \equiv \sqrt{(\Delta\eta)^2 + (\Delta\phi)^2} = 0.4$ centered on the lepton, minus the lepton E_T (p_T), is less than 10% of the lepton E_T (p_T) for electron (muon).
- [16] M. L. Mangano, M. Moretti, F. Piccinini, R. Pittau, and A. D. Polosa, J. High Energy Phys. 07 (2003) 001.
- [17] T. Sjostrand, S. Mrenna, and P. Skands, J. High Energy Phys. 05 (2006) 026.
- [18] D. Acosta *et al.* (CDF Collaboration), Phys. Rev. D **71**, 052003 (2005).
- [19] H. L. Lai *et al.* (CTEQ Collaboration), Eur. Phys. J. C **12**, 375 (2000).
- [20] E. A. Gerchtein and M. Paulini, ECONF C0303241, TUMT005 (2003); R. Brun and F. Carminati, CERN Program Library Long Writeup Report No. W5013, 1994.
- [21] K. Cranmer, Comput. Phys. Commun. **136**, 198 (2001).
- [22] T. Aaltonen *et al.* (CDF Collaboration), Phys. Rev. D **79**, 092005 (2009).
- [23] M. Cacciari *et al.*, J. High Energy Phys. 04 (2004) 068.
- [24] C. Loader, *Local Regression and Likelihood* (Springer, New York, 1999).
- [25] R. Barlow, Nucl. Instrum. Methods Phys. Res., Sect. A **297**, 496 (1990).
- [26] F. James and M. Roos, Comput. Phys. Commun. **10**, 343 (1975).
- [27] A. Bhatti *et al.*, Nucl. Instrum. Methods Phys. Res., Sect. A **566**, 375 (2006).
- [28] G. Corcella *et al.*, J. High Energy Phys. 01 (2001) 010.
- [29] A. Abulencia *et al.* (CDF Collaboration), Phys. Rev. D **73**, 032003 (2006).
- [30] J. Pumplin *et al.*, J. High Energy Phys. 07 (2002) 012.
- [31] A. D. Martin *et al.*, Eur. Phys. J. C **14**, 133 (2000).
- [32] M. Cacciari *et al.*, J. High Energy Phys. 04 (2004) 068.
- [33] D. Wicke and P. Z. Skands, Eur. Phys. J. C **52**, 133 (2007).
- [34] R. Field and R. C. Group, arXiv:hep-ph/0510198v1.
- [35] A. Abulencia *et al.* (CDF Collaboration), Phys. Rev. Lett. **102**, 152001 (2009).
- [36] V. M. Abazov *et al.* (D0 Collaboration), Phys. Rev. D **80**, 092006 (2009).